Indian Journal of Biochemistry & Biophysics
Vol. 62, December 2025, pp. 1429-1442
DOI: 10.56042/ijbb.v62i12.7010

Phyto-fabrication and characterization of silver nanoparticles from *Trachyspermum ammi* (Ajwain) seeds and assessment of their antifungal activity

Malleswara Rao Peram[1], Sunil Attimarad[2], Vijay M Kumbar[3], Vidyadhara Suryadevara[1], Chakravarthy Adusumalli[1] & KRS Sambasiva Rao[4]*

[1]Department of Pharmaceutics, Chebrolu Hanumaiah Institute of Pharmaceutical Sciences, Guntur-522 006, Andhra Pradesh, India

[2]Department of Pharmaceutics, Maratha Mandal's College of Pharmacy, Belagavi-590 016, Karnataka, India

[3]Dr. Prabhakar Kore Basic Science Research Centre, KLE Academy of Higher Education and Research (KLE University), Belagavi-590 010, Karnataka, India

[4]Department of Pharmacy, Mangalayatan University- Jabalpur, Jabalpur-483 001, Madhya Pradesh, India

Received 29 November 2023; *revised 02 September 2025*

The rising incidence of fungal infections combined with the emergence of resistance to existing antifungal drugs highlight the urgent need for novel, safe, and eco-friendly therapeutic options. Green nanotechnology provides a sustainable way to build such alternatives. The present study reports an inexpensive, environmentally acceptable, and non-toxic green method for the biosynthesis of silver nanoparticles (AgNPs) utilizing aqueous seed extract of *Trachyspermum ammi* (TA). The biosynthesized *T. ammi*AgNPs (TA-AgNPs) were characterized using several sophisticated analytical techniques, and their antifungal efficacy was studied. The formation of AgNPs was visually represented by a shift from a light brown to a dark or red-brown color and confirmed by the surface plasmon resonance band at 419 nm. The particle size, polydispersity index, and zeta potential of AgNPs were found to be 101.5 nm, 0.270, and – 41.7 mV respectively. Studies using a transmission electron microscope (TEM), energy dispersive X-ray spectroscopy (EDX), selected area electron diffraction (SAED) spectrum, and X-ray diffraction (XRD) confirmed that the biosynthesized AgNPs were spherical, contained elemental silver, and had a crystalline structure. The TA-AgNPs showed distinctive antioxidant potential, biocompatibility, and promising antifungal activity against *Candida* species and *Aspergillus niger*. The disc diffusion method demonstrated that TA-AgNP's gel had more pronounced antifungal activity than the commercially available Silverex™ ionic (silver nitrate 0.2% *w/w*) gel. In conclusion, the present work showed that TA seed extract mediated AgNPs gel could be the potential therapeutic agent for human fungal infections.

Keywords: Antioxidant, Fungal infection, Green synthesis, Hemocompatibility, Nanogel

Fungi, which were previously considered to be non-infectious to humans, are now found in greater numbers among opportunistic pathogens. Due to their flexibility to a huge range of environmental conditions, these fungi became dangerous to the lives of immunocompromised patients[1]. Over 150 million serious fungal infections take place worldwide each year, resulting in 1.7 million fatalities[2]. Currently, there are approximately 80 types of antifungal agents used in clinics. The major groups of clinically used antifungal agents are β-glucan synthesis inhibitors (echinomycin), ergosterol synthesis inhibitors (azoles, and morpholines), and agents that alter the function of the fungal cell membrane (polyenes), pyrimidine analogs, and allylamines[3]. However, in recent years the resistance of opportunistic pathogens has increased due to the overuse of these antifungal agents[4]. As a result, new treatment strategies are required to address this problem, as well as to overcome the side effects, toxicity, and medication interactions associated with currently available antifungal drugs, all of which may restrict therapy effectiveness[3].

In recent years, nanotechnology has evolved as one of the interesting strategies to overcome the problems and to increase the potency and efficiency of conventional antifungal agents[5]. Metallic nanoparticles are already proven as ideal candidates to control a variety of pathogens. Among the metallic nanoparticles, silver nanoparticles (AgNPs) have a variety of applications in the biomedical field. Though AgNP's are non-toxic to animal cells, their toxicity towards bacterial cells makes them an

*Correspondence:
Phone: +91-7630079075 (Mob)
E-mail: krssrao@yahoo.com

effective and safe bactericidal agent. AgNPs are also known to have antioxidant, anti-inflammatory, anti-bacterial, anti-viral, anti-fungal, and anti-cancer properties[6]. Nanoparticles are typically produced using one of three methods: physical, chemical, or biological synthesis. The physical method requires a large amount of energy and sophisticated laboratory equipment, which makes it costly, whereas chemical synthesis usually requires the use of highly toxic chemicals. Biological or green synthesis, which makes use of microorganisms such as bacteria, algae, fungus and plants,is favored over physical and chemical processes due to its low environmental impact and affordability[6]. Plant (Phyto) mediated fabrication of AgNPs has gained popularity among the other green approaches since it is easily available in large quantities, contains secondary metabolites, and has negligible cross-contamination between plant extracts[7]. Hence in the present study, *Trachyspermum ammi* was selected for fabrication of AgNPs.

Trachyspermum ammi (TA) popularly known as Ajwain is a highly valued medicinal seed spice belonging to the *Apiaceae* family. It is a well-known ayurvedic medicine for its anti-diarrheal, anti-microbial, anti-fungal, anti-viral, anti-spasmodic, broncho-dilating, anti-ulcer, hepatoprotective, anti-hypertensive, anti-hyperlipidemic, detoxification, anti-oxidant and digestive stimulant activity[8]. The bioactive secondary metabolites found in plants, such as phenols, flavonoids, quinones, coumarins, xanthones, saponins, alkaloids, polypeptides, terpenoids, and essential oils are responsible for antifungal activity[9]. The seeds of the plant were reported to contain thymol, para cymene, α and β- pinene, α and γ- terpinene, carvacrol, glycosides, tannins, saponins, and flavones[10]. Among these, the major active phytoconstituents thymol (35-60%) which is a phenol derivative of natural mono-terpenoid reported to have antifungal, antispasmodic, and germicidal properties[8].

The available literature reports few studies on the biosynthesis of silver[11], gold[12,] and selenium nanoparticle[13] using TA leaves and seed extract. Most of these studies are focused either on size-controlled synthesis of stable AgNPs[14] or evaluation of antimicrobial[15], anticancer[16], anti-rheumatic[13], biofilm inhibition, and catalytic reduction activities[17]. However, none of the studies reported the anti-fungal activity of AgNPsphyto-fabricated with aqueous seed extract of TA. Hence the main objective of the present research work is to biosynthesize AgNPs using TA seed aqueous extract and characterize them using ultraviolet-visible (UV-Visible) spectroscopy, Fourier transform infrared spectroscopy (FTIR), zeta sizer, transmission electron microscope (TEM), energy dispersive X-ray spectroscopy (EDX), selected area electron diffraction (SAED) spectrum, and X-ray diffraction (XRD). The synthesized AgNPs were tested for *in vitro* anti-oxidant, anti-fungal, and cytotoxic activities. Finally, the AgNPs were incorporated into a topical gel base and evaluated for their antifungal activity against four different fungi by comparing it with the commercially available Silverex™ ionic (silver nitrate gel 0.2% *w/w*).

Materials and Methods

Materials

Silver nitrate ($AgNO_3$) and sodium hydroxide (NaOH) were provided by S.D. Fine Chem. Limited, located in Mumbai, India. Fluconazole, Brain Heart Agar (BHA), and Sabouraud Dextrose Agar were acquired from Hi Media Laboratories Pvt. Ltd. in Mumbai, India, respectively. Carbopol-934 and triethanolamine were obtained from LobaChemPvt. Ltd. in Mumbai. Methyl and propylparaben were purchased from Sigma Aldrich, Bangalore, India. TA seeds were procured from a nearby market situated in Belagavi, Karnataka, India. Milli-Q ultrapure water was used for all the experiment.

Preparation of aqueous seed extract of TA

The TA seeds were washed with milli-Q water to remove any remaining dust and then air-dried before being ground into a powder in an electric grinder. Ten grams of seed powder was taken in a conical flask containing 100 mL of Milli-Q water, stirred thoroughly, and heated at 100°C for 15 min. The cooled extract was filtered through muslin and then Whatman no. 1 filter paper. The obtained extract was then stored at 4°C. The qualitative phytochemical analysis of the plant extract was performed using standard experimental methods to identify the various phytoconstituents contained in the extract[18].

Green synthesis of *T. ammi*silver nanoparticles (TA-AgNPs)

The prepared aqueous TAseed extract (5 mL) was mixed with 45 mL of 2 mM aqueous $AgNO_3$ solution and the pH of the reaction mixture was brought up to 9 at room temperature (25 ± 2°C) by using 1 % *w/v* NaOH solution with constant stirring. The reduction of Ag^+ ions to AgNPs was confirmed by a

color alteration from pale yellow to dark brown. The prepared AgNP's were centrifuged for 25 min at 10,000 rpm at 4°C. The pellet obtained was washed and resuspended in the Milli-Q water and subjected to centrifugation again. This purification step was repeated three times to remove any residues of the extract. Finally, the purified AgNPs obtained as the pellet was dried (40°C) into a fine powder and used for further characterization[19]. The schematic diagram showing the green synthesis of AgNPs using aqueous TA seed extract is shown in (Fig. 1).

Characterization of TA-AgNPs

UV-Visible spectroscopy

The process of reducing silver ions to nanoparticles was studied by recording the absorption spectra of AgNPs in the 200-800 nm range with a UV-visible spectrophotometer (UV-3200, Labindia Analytical, India)[13].

FTIR

The FT-IR spectra of synthesized TA-AgNPs and aqueous TA seed extract powder were obtained using an FT-IR spectrophotometer (IR Affiity-1S, Shimadzu, Japan)[13]. The samples were thoroughly mixed with potassium bromide (KBr) and FT-IR spectrums werecollected in the range of 4000 – 400 cm^{-1}.

XRD

An X-ray diffractometer (Bruker, Germany) with a Cu-Kα radiation source, operating at 40 kV voltage and 40 mA current, with a 2θ range of 20° to 80°, was used to produce the X-ray diffraction pattern of the biosynthesized TA-AgNPs[16].

TEM, EDX, and SAED

The morphological properties, including the size and shape of TA-AgNPs, were examined using a transmission electron microscope (TEM) that operates at an accelerating voltage of 300 kV. Following 5 min sonication, the sample was placed on carbon-coated copper grids to air dry. Images were taken at different magnifications. EDX and SAED were used to determine the elemental composition and crystalline structure of synthesized AgNPs respectively[14].

Particle size, polydispersity index (PDI)and zeta potential (ZP)

The synthesized TA-AgNPs' particle size, PDI, and ZP were determined by a Zetasizer Nano ZS instrument (Malvern Instruments Ltd., U.K.). The size and ZP of TA-AgNPs were measured by using the Dynamic light scattering method (DLS) and the M3-PALS (phase analysis light scattering) technique, respectively. For determination, the synthesized AgNPs were dispersed in Milli-Q water, bath sonicated for 5 min and measurements were carried out at ambient temperature[14].

***In vitro* antioxidant assays**

DPPH free radical scavenging activity

The DPPH free radical scavenging assay was carried out following the method published in the literature with slight modifications[20]. Aliquots of different concentrations (2.5, 5,10, 20, 40, and 80 µg/mL) of aqueous seed extracts of TA and

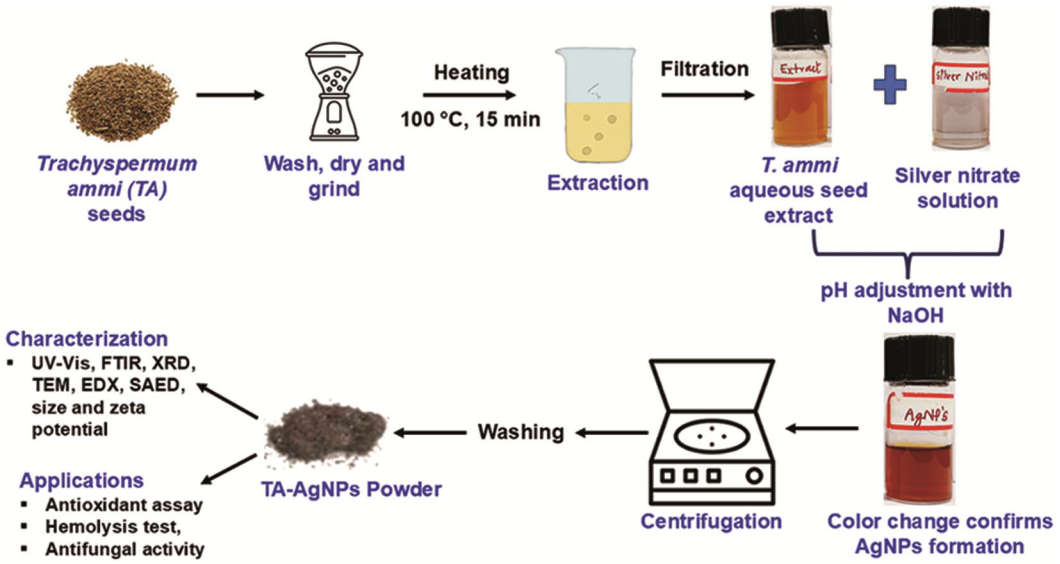

Fig. 1 — Schematic diagram illustrating the green synthesis of silver nanoparticles from *Trachyspermum ammi* aqueous seed extract

TA-AgNPs were mixed with 3 mL of methanol containing 0.1 mM DPPH radicals. The reaction mixture was incubated in a dark place for 30 min at room temperature. Following incubation, 250 µL of supernatant was transferred into 96 well microplate and absorbance was measured at 517 nm using ELISA reader. The DPPH solution without the TA extract and TA-AgNPs was served as control and methanol was used as blank. The standard utilized was ascorbic acid. The following formula was used to compute the radical scavenging activity, which is evaluated as % inhibition. [(Absorbance of control-absorbance of test)/Control absorbance] x 100. A graph was plotted by taking concentration against percentage inhibition and IC_{50} values were obtained using Graph pad prism program.

Ferric reducing antioxidant power (FRAP) assay

Different concentrations of aqueous seed extracts of TA and TA-AgNPs, ranging from 5 to 80 µg/mL, were treated with a solution containing 2.5 mL of 1% *w/v* potassium ferricyanide and 2.5 mL of phosphate buffer (20 mM). The resulting mixture was then kept for 30 min at a temperature of 50°C. To the aforementioned solution, 2.5 mL of trichloroacetic acid (10% *w/v*) and 0.5 mL of ferric chloride (0.1% *w/v*) were introduced and allowed to incubate for 10 min. The absorbance measurement was conducted using a UV-visible spectrophotometer at 700 nm. The experimental standard used was ascorbic acid[20].

Phosphomolybdenum Assay (PM)

Different concentrations of aqueous seed extracts of TA and TA-AgNPs, ranging from 5 to 80 µg/mL, were separately added to each test tube containing a mixture of distilled water and Molybdate reagent in a ratio of 3:1. The tubes were subjected to incubation at a temperature of 95°C for 90 min. After 90 min, the tubes were allowed to return to ambient temperature for the duration of 20 to 30 min, following which the absorbance was quantified at 700 nm. The experiment included ascorbic acid as the standard[20].

***In-vitro* antifungal activity of TA-AgNPs**

The antifungal activity of the synthesized TA-AgNPs was evaluated against a variety of pathogenic strains, including *Candida albicans* (ATCC10231), *Candida parapsilosis* (ATCC22019), *Candida tropicalis* (ATCC750) and *Aspergillus niger* (ATCC66275).

***Minimum inhibitory concentration* (*MIC*)**

To ascertain the MIC of TA-AgNPs against the test fungal pathogens under investigation, a 96-well microtitre plate was employed. A two-fold dilution of the TA-AgNPs (ranging from 0.20 to 100 µg/mL) was prepared using an autoclaved medium on a 96-well microtitre plate. Each well was inoculated with 10 µL of the 12 h developed culture, whereas the control group, which did not include TA-AgNPs, was incubated overnight. The visible turbidity of the tubes before and after incubation is taken into consideration when calculating the MIC[21].

***Minimum Bactericidal Concentration* (*MBC*)**

The micro broth dilution method was employed to conduct the MBC test for TA-AgNP's. Two-fold dilutions of different concentrations (0.20- 100 µg/mL) of the TA-AgNPs were made for treatment. To ascertain the minimum bactericidal concentration (MBC), cultures that had been cultivated for 12 h were streaked onto agar plates containing different concentrations of the TA-AgNPs. The MBC endpoint is the lowest amount of an antimicrobial agent needed to eradicate roughly 99.9% of the initial bacterial population[21].

Agar well diffusion assay

The antifungal activity of the TA-AgNPs was determined by the utilization of the agar well diffusion test. The microorganisms were cultivated in the nutritional broth overnight to achieve a colony-forming unit (CFU) count of around ~10^6 per milliliter. A volume of 100 µL from each fungal culture was applied to the agar plates. The agar wells (8 mm in diameter) were punctured using sterilized micropipette tips and subsequently filled with TA seed extract, $AgNO_3$ solution, a standard antibiotic (fluconazole), and TA-AgNP's using micropipette tips. The plates are thereafter placed in an incubator and allowed to incubate for a period of 24 to 48 h at 37°C. The sizes of the inhibitory zones were measured and recorded in millimeters (mm)[22].

Hemolysis assay of AgNPs

The hemocompatibility of the TA-AgNPs was assessed using a hemolysis assay, using a previously reported protocol with minor adjustments[23]. A sample of blood was obtained from a healthy donor in a heparinized tube to prevent coagulation. The red blood cells (RBC) were isolated with the addition of a lymphocyte separation reagent (Hisep-LSM-1077), followed by centrifugation at a reduced speed for 30

min. The pellet of red blood cells (RBCs) was thereafter rinsed multiple times with a Phosphate buffer solution (PBS) at a pH of 7.4. Following this, the RBCs were dispersed in 40 mL of PBS to create a suspension for the hemolysis assay. A volume of 200 µL of RBC suspension was separately introduced into varying concentrations of TA-AgNPs (5, 10, 50, and 100 µg/mL), as well as a 2% Triton-X solution (serving as the positive control). The liquid portion produced after subjecting a suspension of RBC (without TA-AgNPs and Triton-X) to centrifugation was designated as the blank. The samples are incubated for 3h at ambient temperature. The morphological alterations in red blood cells (RBCs) were examined by applying a 10 µL sample of the cells onto a glass slide that was free of grease, and thereafter observing them using a microscope. Following the incubation period, the mixture was subjected to centrifugation at 5,000 rpm for 5 min at 4°C. The absorbance of the resulting supernatant was measured at a wavelength of 560 nm using a microplate scanning spectrophotometer (BIO RAD iMark™). The experiment was conducted in duplicate, and the percentage of hemolysis was calculated using the following formula.

$$\%\text{Hemolysis}=\frac{\text{sample absorbance - blank absorbance}}{\text{positive control absorbance - blank absorbance}}\times 100$$

Preparation of TA-AgNPs gel

The TA-AgNPs gel was made by accurately weighing the required amount of carbopol-934 and dispersing it in a beaker containing 8 mL of distilled water. The beaker was set aside overnight at 4°C to facilitate the swelling of the polymer. The required amount of TA-AgNPs was introduced into the carbopol dispersion while swirling continuously until the AgNPs were fully dispersed. Both methyl paraben and propyl paraben were included in the aforementioned dispersion. Subsequently, the volume was adjusted to 10 mL using distilled water, and triethanolamine was incrementally introduced into the formulation to get the desired gel consistency[24].

Evaluation of TA-AgNPs gel

A visual examination was performed on the TA-AgNPs gel to check for color, consistency, and phase separation. The pH of the TA-AgNPs gel was determined by placing the glass electrode in the gel and taking a reading. The viscosity was evaluated at 25°C using a cone and plate Brookfield viscometer (Brookfield Engineering Laboratories, USA) utilizing spindle No.1. With the help of the spatula, 0.1 g of gel was deposited in the middle of the viscometer plate directly below the spindle, and its viscosity was measured while spinning at 50 rpm. The spreadability of TA-AgNPs gel (g.cm/s) was assessed by placing the formulation onto glass slides with a length of 6 cm and applying a weight of 20 g. The time in seconds taken for the slides to separate was then recorded. The spreadability was determined by utilizing the following formula[25].

$$S = (W\times L)/T$$

Where S is spreadability, W is the weight applied to the upper slide, L is the length of the glass slide and T is time in seconds.

***In vitro* antifungal activity of TA-AgNPs gel by disc diffusion studies**

The evaluation of the antifungal efficacy of the TA-AgNPs gel was conducted using the agar well disc diffusion method. The pure cultures of fungal pathogens were sub cultured in brain heart infusion broth (BHI). With the use of sterile cotton swabs, each strain was evenly distributed over the separate plates. Wells with a diameter of 5 mm was created on the brain heart infusion agar plate. A micropipette was employed to dispense 50 µL of the 0.2% TA-AgNPs gel sample and the commercially available Silverex™ ionic (0.2 % *w/w* $AgNO_3$ gel) onto each well of all the plates. The plates were subjected to incubation at 37°C for 24 h. After 24 h, the zones of inhibition were measured[22].

Statistical analysis

Data was statistically analyzed using GraphPad Prism (GraphPad Software Inc., CA, USA). *In-vitro* antioxidant assay and agar diffusion anti-fungal assay results were examined using two-way *ANOVA* with Tukey's multiple comparison test. The IC_{50} values were computed using GraphPad Prism software by logarithmic transformation of the inhibitor versus response data. P-values below 0.05 were statistically significant. The % haemolysis assay results were analysed using one-way ANOVA with Sidak's multiple comparison test.

Results and discussion

Phytochemical analysis

The phytochemical analysis of aqueous TA seed extract showed the presence of alkaloids, carbohydrates, flavonoids, terpenoids, tannins, inorganic acids, proteins, and amino acids (Table 1).

Similar results were previously reported in the phytochemical profiling of *T. ammi* crude extract used for the synthesis and bioactivity studies of gold nanoparticles[12]. Various biomolecules and secondary metabolites such as proteins, carbohydrate, amino acids, vitamins, terpenoids, flavonoids, polyphenols, and alkaloids present in the plant extract plays a key role in the green synthesis of AgNPs by acting as reducing and stabilizing agent. These biomolecules are responsible for donating electrons to reduce the Ag^+ to Ag^0 and organize the Ag^0 into AgNPs[26].

Characterization TA-AgNPs

Visual observation

The formation of AgNPs is confirmed by visual observation of color change from pale yellow to dark brown (Fig. 2). The change in the color of the aqueous TA seed extract from pale yellow to dark brown after the addition of $AgNO_3$ solution is caused by the reduction of silver ions to AgNPs. Similar types of color changes were observed during the green synthesis of AgNPs from *Tectona grandis* seeds extract[21] and pomegranate leaf extract[19].

UV-Visible spectroscopy

UV-visible spectroscopy is an efficient technique to confirm the formation of metal nanoparticles in aqueous solutions. AgNPs are known to exhibit a surface plasmon resonance (SPR) band in the range of 400-500 nm due to the excitation of free electrons in response to the incident light[27]. The location of the SPR band also provides information about the size of the synthesized nanoparticles. A peak shift towards a shorter wavelength (blue shift) or narrow absorption peak indicates small-sized AgNPs whereas a shift towards a longer wavelength (redshift) and a broader peak indicates large-sized AgNPs[27]. The UV-visible spectrum of AgNPs synthesized from aqueous seed extract of TA is shown in (Fig. 2). The spectrum shows the characteristic SPR peak at 419 nm confirming the formation of AgNPs with smaller size. Similar types of peaks were observed previously for *Punica granatum*[19] and *Leea indica* AgNPs[20].

Table 1 — Phytochemical analysis of aqueous TA seed extract

S. No	Phytoconstituents	Results
1	Alkaloids	+
2	Carbohydrates	+
3	Flavonoids	+
4	Glycosides	-
5	Steroids	-
6	Terpenoids	+
7	Tannins	-
8	Inorganic acids	+
9	Protein	+
10	Amino acid	+

'+' indicate presence of phytoconstituents, '-' indicate absent

FTIR

FTIR is an efficient technique to identify the phytoconstituents responsible for the reduction and stabilization of AgNPs. The active functional groups found in the phytoconstituents including the -OH, $-NH_2$, and -CHO were oxidized by the silver ions. A small shift in the position or absence of bands is regarded as the indication of the reduction of metal ions and formation of nanoparticles[27]. The FTIR spectrum of aqueous TA seed extract powder and TA-AgNPs are presented in (Fig. 3A). The FTIR spectra of aqueous seed extract of TA shown peaks at 3376, 2931, 2123, 1655, 1407, 1049, and 864 cm^{-1} corresponding to stretching vibrations of –OH of

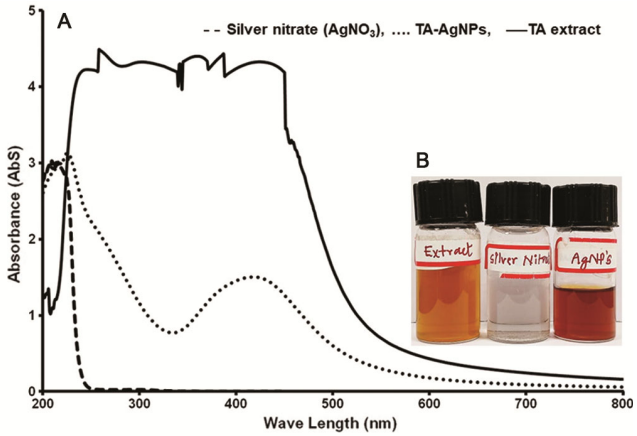

Fig. 2 — UV-Vis absorption spectra of TA-AgNP's, (A) TA seed extract and 2mM silver nitrate, and (B) Visual observation of colour change of TA seed extract, silver nitrate, and TA-AgNPs in solution

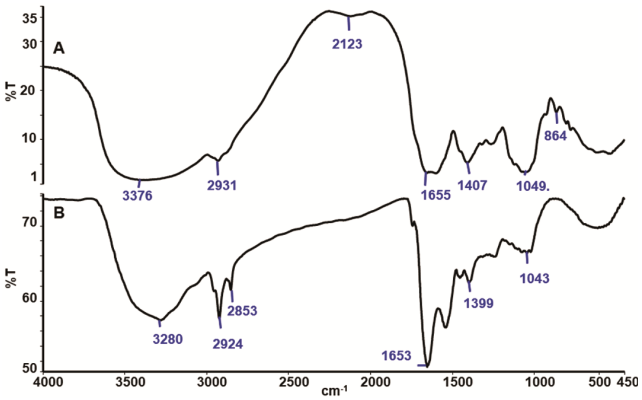

Fig. 3 — FTIR spectra of aqueous (A) TA seed extract, and (B) TA-AgNPs

phenols, C-H of alkanes, C=C of proteins, C=O of flavone, C=C of alkyne, C-O and N-H of amines respectively. Compared with aqueous TA seed extract, the TA-AgNPs spectrum (Fig. 3B) showed a small shift in the peaks (3376 -3280 cm^{-1}, 2931- 2924 cm^{-1}, 1655- 1653 cm^{-1}, 1407-1399 cm^{-1} and 1049 to 1044 cm^{-1}). Further, the peaks at 2123 and 865 cm^{-1} were completely disappeared. These results suggest that –OH, C-H, C=O, C=C, and N-H groups present in the phytoconstituents were accountable for the reduction of silver ions and the formation of AgNPs. These results are in good agreement with previous studies that reported the involvement of -OH in the formation of AgNPs using the green synthesis method. The -OH group of phenols donates an electron to reduce Ag+ and hence act as a reducing agent and the carbonyl and primary amine group of protein can bind the metal surface. Hence, they act as capping and stabilizing agent[15].

XRD

XRD pattern analysis was used to confirm the crystalline structure of the synthesized AgNPs. The XRD spectrum of TG-AgNPs is shown in (Fig. 4). Four diffraction peaks were observed at 2θ values of 38.11°, 46.92°, 65.20° and 77.70° that were indexed to (111), (200), (220) and (311) planes respectively. The presence of diffraction peaks and their reflection planes indicated that the synthesized TA-AgNPs were crystalline with a face-centered cubic (FCC) structure. The present findings were in good agreement with the previous studies for AgNPs synthesized using *Perilla frutescens* leaf extract[28] and *Tectona grandis* seeds extract[22].

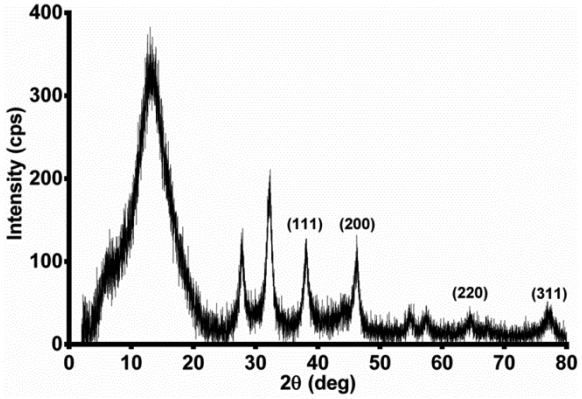

Fig. 4 — XRD pattern of AgNP's synthesized by TA aqueous extract

TEM, EDX and SAED

TEM is used to analyze the size, shape, and morphological characteristics of the synthesized Ag-NPs. The TEM image of TA-AgNPs is shown in (Fig. 5A). The synthesized AgNPs were predominantly spherical, with a size ranging from 15-26 nm, and well dispersed with few traces of clusters. Our TEM results were consistent with previously published reports[21]. EDX is employed to ascertain the elemental composition and purity of the AgNPs. The EDX spectra (Fig. 5B) of TA-AgNPs depicted a sharp peak located at 3 keV confirming the presence of silver in the synthesized AgNPs. The Ag element accounted for 96.40 % of the total weight composition. EDX also revealed the presence of some minor peaks corresponding to other elements such as oxygen (O) and nitrogen (N). These may be due to the presence of moieties of phytoconstituents which are involved in the capping and stabilization of AgNPs. Similar results were obtained for AgNPs synthesized using aqueous fruit shell extract of *Tamarindus indica*[29]. In addition to XRD, the SAED pattern is also used to determine the crystalline structure of AgNPs. The SAED pattern displayed four circular bright rings indexed to (111), (200), (220), and (311) are the characteristic reflection of the face-centered cubic crystalline structure of silver (Fig. 5C). The findings of the present study comply with other published reports[30].

Particle size, PDI and ZP

The particle size, PDI, and ZP of TA-AgNPs were determined by a Zetasizer instrument. The DLS

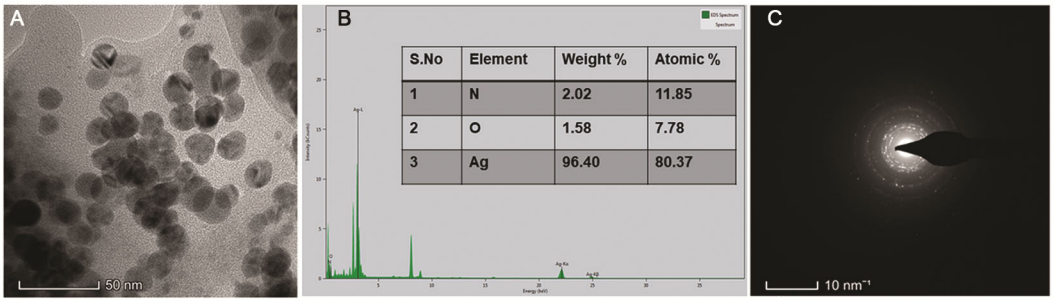

Fig. 5 — (A) TEM image, (B) EDX spectra, and (C) SAED pattern of synthesized TA-AgNPs

technique is used for the measurement of hydrodynamic size whereas the M3-PALS (phase analysis light scattering) technique is used to determine the electrophoretic mobility of AgNPs. The size, PDI, and ZP of the TA-AgNPs were found to be 101 nm, 0.270, and - 41.7 mV respectively (Fig. 6A & B). The particle size obtained from the Zetasizer was found to be bigger when compared to the TEM. The difference in particle sizes measured by TEM (15–25 nm) and DLS (101 nm) is a commonly reported phenomenon in nanoparticle characterization. TEM assesses the actual metallic core diameter in its dried state, while DLS evaluates the hydrodynamic diameter in suspension, comprising the metallic core, surface-attached phytochemicals from *T. ammi* extract, and the associated solvation layer. Furthermore, as DLS provides an intensity-weighted distribution, larger particles or small aggregates significantly influence the measurement (because scattering intensity is proportional to the sixth power of particle radius), thus overestimating the mean hydrodynamic size. Even in minimal proportions, these larger particles can obscure the influence of smaller nanoparticles and increase the average size. An additional factor contributing to this discrepancy is the radius of curvature effect: smaller nanoparticles, due to their higher surface curvature, adsorb a greater quantity of phytochemicals, ions, and water molecules, resulting in a thicker solvation/capping layer that increases the hydrodynamic diameter measured by DLS in contrast to the core size observed by TEM[31,32]. The PDI value 0.270 indicates that the distribution of TA-AgNPs was monodisperse. The ZP measurement gives valuable information about the surface charge and the ultimate stability of AgNPs. The ZP values greater than + 30 mV or – 30 mV indicate the high stability of AgNP colloidal dispersion. The TA-AgNP's ZP value of -41.7 mV specifies that synthesized nanoparticles are extremely stable with no aggregation due to strong electrostatic repulsive forces between the particles. The present study findings were consistent with the previous reports where higher negative ZP values of -67.2 mV[19], and -33.8 mV were obtained for AgNPs synthesized from pomegranate leaf[19] and walnut green husk extract[33].

In vitro antioxidant assays

An overabundance of reactive oxygen species (ROS) in the body has been implicated in numerous disorders, including cancer, aging, cataracts, diabetes, heart disease, and brain disorders. Antioxidants are vital in disease prevention because of their radical scavenging capabilities, which stop free radicals before they damage cells and other biological

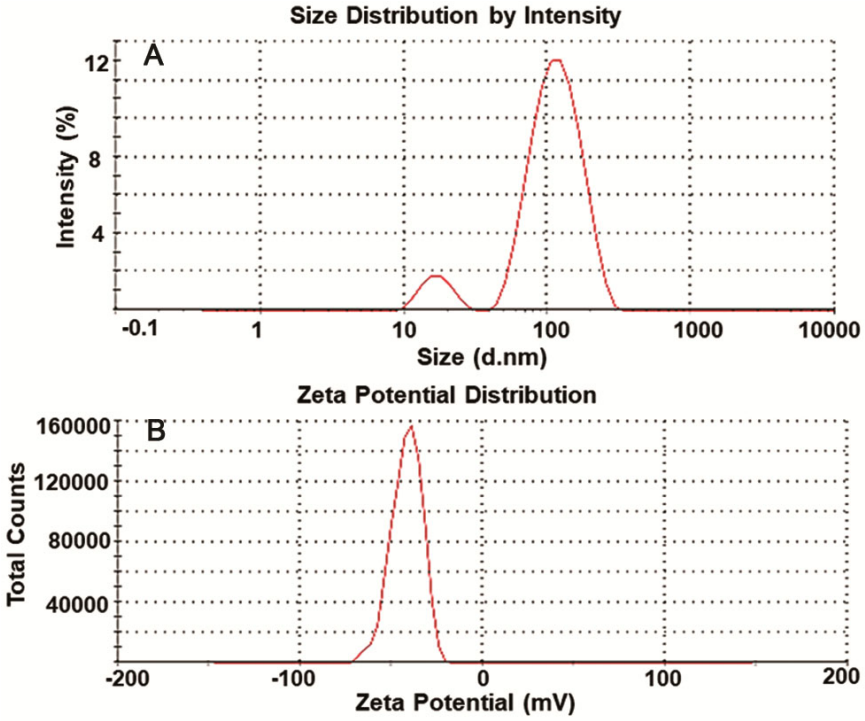

Fig. 6 — Particle size (A), and zeta potential (B) of TA-AgNP's

targets[30]. Three separate assays, DPPH, FRAP, and FM were conducted at concentrations ranging from 2.5 to 80 µg/mL, to provide a precise assessment of the antioxidant capabilities of aqueous TA seed extract and synthesized TA-AgNPs.

DPPH free radical scavenging activity

The most common method for testing the antioxidant potential of plant extract or synthetic compounds is to utilize DPPH, a stable nitrogen-centered free radical[20]. The DPPH scavenging activity of the aqueous TA seed extract and TA-AgNPs is depicted in (Fig. 7A). It is evident from the figure that both aqueous TA seed extract and TA-AgNPs can scavenge free radicals, and their inhibitory action is concentration-dependent. The % inhibition was 81.16 ± 0.98, 70.93 ± 0.32, and 52.32 ± 0.31 for ascorbic acid, TA-AgNPs, and aqueous TA seed extract at 80 µg/mL respectively. Compared to aqueous TA seed extract, TA-AgNPs showed superior DPPH scavenging activity ($P< 0.001$) at all the tested concentrations. One possible explanation for this could be the selective adsorption of antioxidant moieties found in the plant extract onto the nanoparticle surface during the capping and stabilization processes[34]. Nevertheless, compared to the standard ascorbic acid, the percentage inhibition values for TA-AgNPs and TA seed extract were lower. These results were similar to previously published data where *Alpinia katsumadai* seed extract-mediated AgNPs showed better DPPH scavenging activity than that of *Alpinia katsumadai* seed extract[30].

FRAP

The FRAP assay relies on the fast conversion of Ferric cyanide (Fe^{3+}) to Ferro cyanide (Fe^{2+}) by the action of antioxidants found in the plant extract. The reduction caused the test solution to

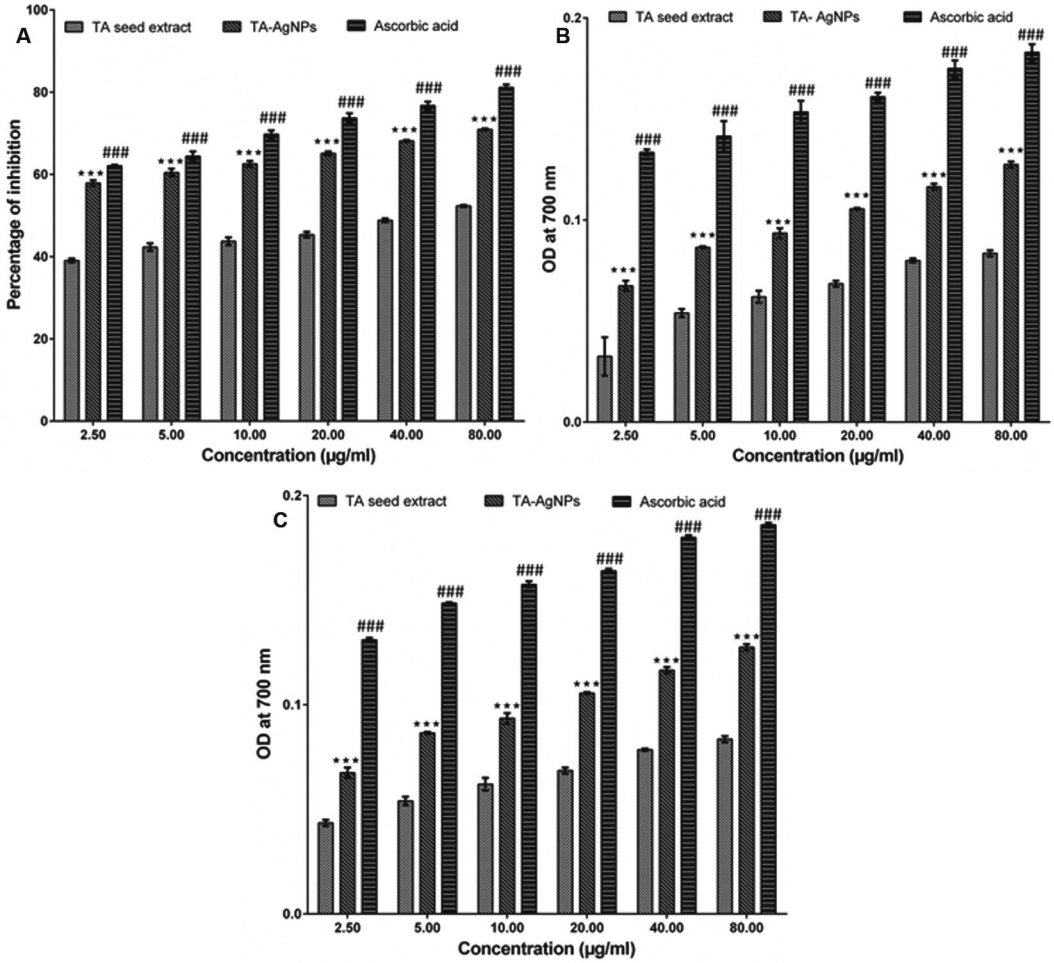

Fig. 7 — *In vitro* antioxidant activity of TA-AgNPs, TA-extract and Ascorbic acid by using (A) DPPH, (B) FRAP; and (C) PM assays. Data are mean ± SD of three independent experiments. Two-way ANOVA was used in the statistical analysis with Tukey's multiple comparison test. Significant difference indicated as *** $P \leq 0.001$ between TA seed extract vs. TA-AgNPs, and; $^{###}P \leq 0.001$ between TA seed extract vs. ascorbic acid

shift color from yellow to a range of blue and green hues which was measured spectrophotometrically at 700 nm[20]. As illustrated in (Fig. 7B), the reducing power of aqueous TA seed extract and TA-AgNPs increased with an increase in the concentration which can be evident from the increase in the absorbance values. However, a significant increase in absorbance values for the TA-AgNPs compared to aqueous TA seed extract at all tested concentration indicate that TA-AgNPs have the highest reducing power. The results were consistent with previous investigations, which found that AgNPs produced from *Prosopis farcta* fruit extract had a much greater reducing power compared to the extract itself[35].

PM

The PM technique was used to assess the total antioxidant activity of the sample. This is a calorimetric quantitative technique that evaluates the reduction in Phosphate-Mo (VI) to Phosphate-Mo (V) caused by the sample, resulting in the development of a bluish-green colored Phosphate-Mo (V) complex. As shown in Fig.7C, absorbance values were increased with an increase in concentration from 2.5-80 µg/mL for TA seed extract, TA-AgNPs, and ascorbic acid. However, the TA-AgNPs exhibited significantly higher antioxidant activity than the TA seed. Similar results have been reported in previous literature[36].

The enhanced antioxidant potential of the phyto-fabricated AgNPs in all three distinct assays could be attributed binding of phytoconstituents such as flavonoids to the surface of AgNPs, their large surface-to-volume ratio and crystalline surface structure[30].

***In-vitro* antifungal activity**

MIC and MBC

The values of MIC and MBC of TA-AgNPs against the test pathogens were mentioned in (Table 2). The values of MIC of TA-AgNPs against test pathogens such as *C. albicans, A. niger, C. tropicalis, C. parapsilosis* were found to be in the range of 0.4 to 1.6 µg/mL. Among all the tested fungi, *C. parapsilosis* was more sensitive (MIC - 0.4 µg/mL) to TA-AgNP's. The pleomorphism and variations in the structural organization of their cell walls could explain the variation in MIC. Literature reports few studies where green synthesized silver nanoparticles from various parts of plant extract showed notable antifungal activity against different fungal species. The MIC values of AgNPs synthesized from *M. oleifera* leaf extract[37] and *Lycopersicon esculentum* extracts[38] against *C. albicans* and *C. parapsilosis* were found to be 6.25µg/mL and 8 µg/mL respectively. The MIC values of tulsi extract mediated AgNPs against the *C. albicans and C. tropicalis* were found to be 60 and 30 µg/mL respectively[39]. Based on the MIC values mentioned earlier, it can be inferred that AgNPs made from aqueous TA seed extract have more efficacy against the tested pathogens compared to AgNPs made from other plant extracts. The MBC values of TA-AgNPs were found to be in the range of 3.2 µg/mL to 50 µg/mL against *C. albicans, A. niger, C. tropicalis, C. parapsilosis.* After taking the MIC and MBC values into account, the optimal concentration for disc diffusion studies was determined to be 50 µg/mL, which can effectively kill the tested pathogens.

Agar well diffusion method

The TA-AgNP's were analyzed for their antifungal activity against *C. albicans, A. niger, C. tropicalis, and C. parapsilosis* by disc diffusion method. The results obtained are shown in (Table 2). By comparing the zone of inhibition, it was observed that TA-AgNPs showed a larger zone of inhibition than TA seed extract and silver nitrate, which implies the significant antifungal activity of TA-AgNPs on all test pathogens. This may be attributed to the smaller size to larger surface area ratio of AgNPs. Smaller AgNPs (10 nm) had a greater lethal impact on microbes than

Table 2 — MIC and MBC of biosynthesized TA-AgNPs and zone of inhibition (mm) of TA-AgNPs, silver nitrate, aqueous TA seed extract and fluconazole

S. No	Fungi	MIC (µg/mL)	MBC (µg/mL)	Zone of Inhibition (mm)			
				TA-AgNP's	Silver nitrate	TA seed extract	Fluconazole
1	*C. albicans*	0.8	6.25	12	10	R	30
2	*C. Parapsilosis*	0.4	50	15	13	R	35
3	*C. Tropicalis*	1.6	25	15	12	R	40
4	*A. niger*	0.8	3.2	18	10	R	25

MIC – minimum inhibitory concentration, MBC - minimum bactericidal concentration, TA-AgNPs - *Trachyspermum ammi* silver nanoparticles, R- resistant

larger ones (20-80 nm), according to earlier research. Cell membranes can be easily penetrated by AgNPs of lower sizes[40]. The AgNPs' antifungal action is probably related to the generation and build-up of free radicals and reactive oxygen species, which can harm cell walls, metabolic pathways within cells, and proteins on the surface of cells, or even nucleic acids[41,42]. However, it is still necessary to investigate the precise mechanism of AgNPs.

Hemolysis assay

Blood can transport foreign substances to cells, tissues, and organs. Hence, it is required to study the nano-toxicity of AgNPs in blood, particularly on red blood cells (RBC). Hemolysis assay was performed to study the hemocompatibility nature of the biosynthesized AgNPs. The percentage hemolysis of TA-AgNPs at different concentrations (5, 10, 50, and 100 µg/mL) on red blood cells is presented in (Fig. 8D). TA-AgNPs showed hemolysis activity in dose dose-dependent manner. At a lower dose (5 µg/mL) it showed 0 % hemolysis, at a dose (10 µg/mL) it showed 2.12 %, at a dose (50 µg/mL) it showed 7.31 % hemolysis and at a higher dose (100 µg/mL) it showed 19.19 % hemolysis. In order to assess the hemocompatibility of a material, the degree of hemolysis can be classified into distinct groups, namely extremely hemocompatible (less than 5% hemolysis), hemocompatible (between 5% and 10% hemolysis), and non-hemocompatible (more than 20% hemolysis)[43]. Thus, the current study findings indicate good hemocompatibility of TA-AgNPs. These results were further supported by morphological observations of RBC under microscope. Figure 8B illustrates that the RBC shape is not adversely altered by TA-AgNPs (100 µg/mL); instead, the membrane remains intact, much like in the control cells (Fig. 8A). However, RBC treated with Triton X are wrinkled and ruptured to liberate haemoglobin (Fig. 8C). Similar results were reported by previous study where extract of crushed, wasted, and spent *Humuluslupulus* stabilized AgNPs exhibited excellent hemocompatability up to 500 µg/mL concentration[43].

Evaluation of gel

The prepared gel was homogenous, clear and free from any particulate matter, clumps and aggregates. The formulated TA-AgNPs gel pH was determined to be 6.7 which are near to the skin pH hence it is

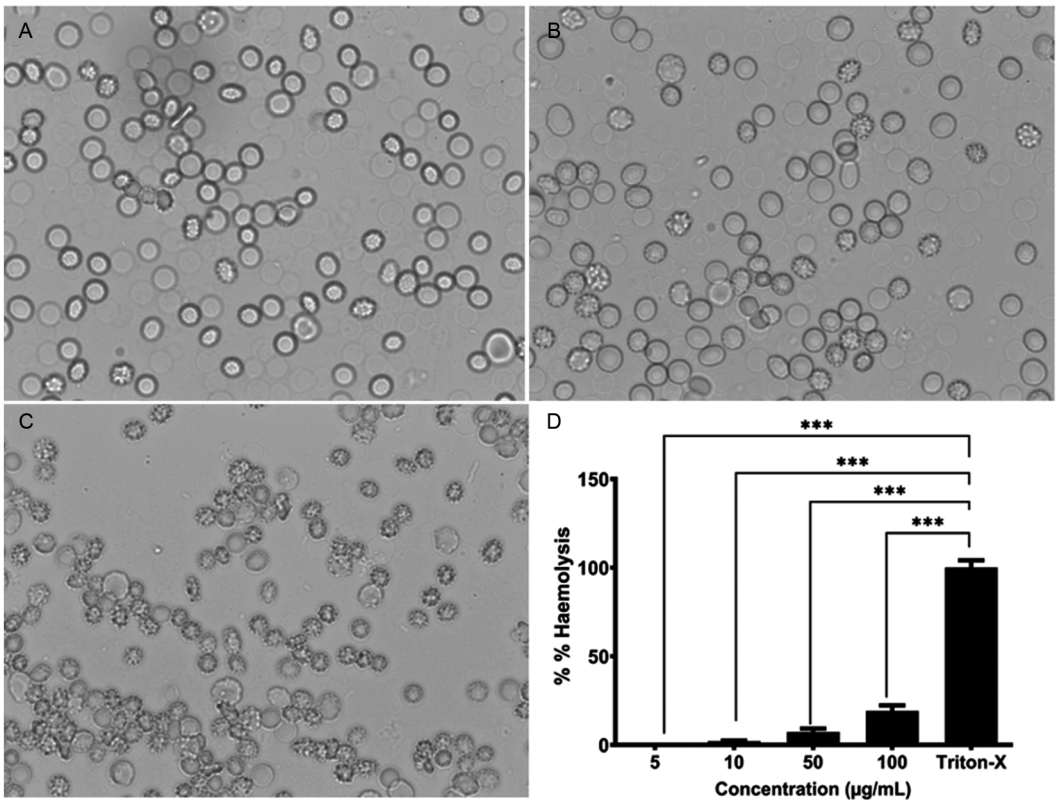

Fig. 8 — Microscopic images of human RBC. (A) Untreated negative control; (B) treated with TA-AgNPs; (C) treated with Triton X 100; and (D) % haemolysis assay of TA-AgNPs. One-way ANOVA was used in the statistical analysis with Sidak's multiple comparison test. Significant difference indicated as *** P<0.001 between TA-AgNP at different concentrations and Triton-X

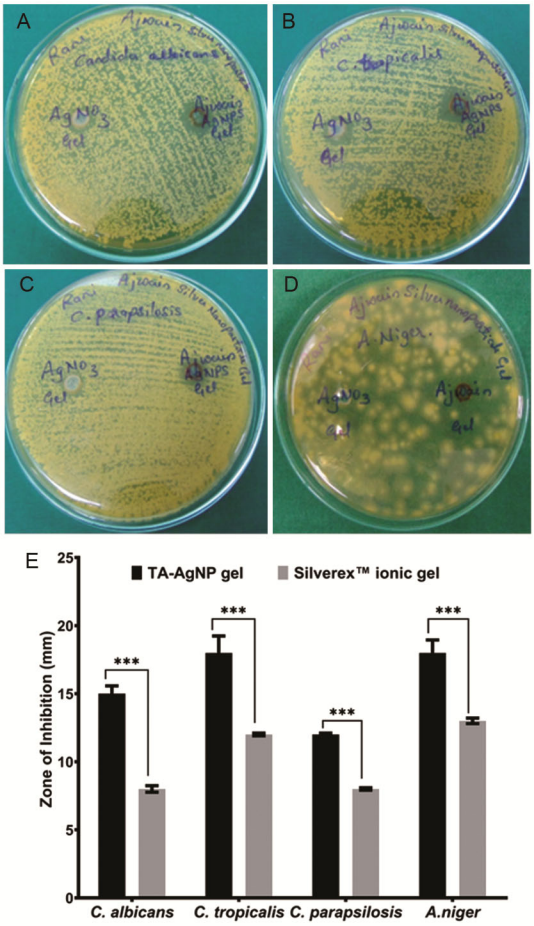

Fig. 9 — Agar diffusion anti-fungal assay of the TA-AgNPs and Silverex^{TM} gel on (A) *C. albicans*; (B) *C. tropicalis*; (C) *C. parapsilosis*; (D) *A. niger* and comparative study of zone of inhibition of TA-AgNP gel; and Silverex^{TM} gel; and (E) in different fungal strains. Two-way ANOVA was used in the statistical analysis with Tukey's multiple comparison test. Significant difference indicated as *** P<0.001 between TA-AgNP gel and Silverex^{TM} gel

thought to be compatible with skin. The viscosity of the gel reflects its consistency. The viscosity of the prepared TA-AgNPs gel was found to be 279 ± 2 cps indicating good consistency. The spreadability value TA-AgNPs gel was found to be 23.16 ± 0.51733 g.cm/sec demonstrating it uniform and faster spreadability on to skin[25].

In-vitro anti-fungal activity of TA-AgNPs gel

The *in-vitro* anti fungal activity of the prepared TA-AgNP's gel was performed by agar well diffusion method. The Figure 9 A-E shows the images of zone of inhibitions of TA-AgNP's gel and marketed formulation against *C. albicans, A. niger, C. tropcalis, C. parapsilosis*. The zone of inhibition values for TA-AgNPs gel was observed to be higher than that of the commercial product (Silverex^{TM}). This may be attributed to the good dispersion capability of TA-AgNPs in the gel formulation which helps in the better penetration of nanoparticles into the cell wall of the fungi thereby showing good antifungal activity than the commercial $AgNO_3$ gel[44]. Furthermore *in vivo* studies in animal models need to be conducted to validate the antifungal activity demonstrated *in vitro*, which will provide stronger translational relevance to our findings.

Conclusion

The present study successfully used aqueous TA seed extract, an environmentally safe and eco-friendly method, to phytofabricate silver nanoparticles. The colour change and UV-Vis spectroscopy demonstrated the AgNPs' production. The crystalline structure of the nanoparticles is verified by XRD and SAED, while EDX confirms the presence of the silver element. According to FTIR data, the proteins, phenols, and polyphenols present in aqueous TA seed extracts are crucial for the reduction of silver ions. The TEM analysis confirmed synthesized AgNPs were spherical and has particle size of 15-26 nm. The higher ZP values of -41.7 mV indicate the good stability of synthesized AgNPs. DPPH, FRAP, and PM assays verified the high level of antioxidant activity of TA-AgNPs. The lack of toxicity towards red blood cells confirms the hemocompatibility of the synthesized TA-AgNPs. The gel loaded with TA-AgNPs exhibits good spreadability and consistency. The *in vitro* antifungal studies on different fungal strains confirmed that the TA seed extract-mediated silver nanoparticles and TA-AgNPs loaded gel demonstrated significant antifungal action. Future studies incorporating NMR analysis and *in vivo* animal studies will provide deeper mechanistic insights and enhance the translational significance of our findings.

Acknowledgement

Authors would like to acknowledge Chebrolu Hanumaiah Institute of Pharmaceutical Sciences, Andhra Pradesh, India and Department of Pharmacy, Mangalayatan University- Jabalpur for providing the necessary facilities to carry out the research work.

Conflict of interest

All authors declare no conflict of interest.

References

1 Brown GD, Denning DW, Gow NA, Levitz SM, Netea MG & White TC, Hidden killers: human fungal infections. *Sci Transl Med*, 4 (2012) 165rv13.

2 Kainz K, Bauer MA, Madeo F & Carmona-Gutierrez D, Fungal infections in humans: the silent crisis. *Microb Cell*, 7 (2020) 143.

3 Campoy S & Adrio JL, Antifungals. *BiochemPharmacol,* 133 (2017) 86.

4 Wiederhold NP, Antifungal resistance: current trends and future strategies to combat. *Infect Drug Resist*, 10 (2017) 249.

5 Sousa F, Ferreira D, Reis S & Costa P, Current insights on antifungal therapy: Novel nanotechnology approaches for drug delivery systems and new drugs from natural sources. *Pharmaceuticals*, 13 (2020) 248.

6 Zhang XF, Liu ZG, Shen W & Gurunathan S, Silver nanoparticles: synthesis, characterization, properties, applications, and therapeutic approaches. *Int J Mol Sci*, 17 (2016) 1534.

7 Ahmad S, Munir S, Zeb N, Ullah A, Khan B, Ali J, Bilal M, Omer M, Alamzeb M, Salman SM & Ali S, Green nanotechnology: A review on green synthesis of silver nanoparticles-An ecofriendly approach. *Int J Nanomedicine*, 14 (2019) 5087.

8 Khan N, Jamila N, Ejaz R, Nishan U & Kim KS, Volatile oil, phytochemical, and biological activities evaluation of *Trachyspermum ammi* seeds by chromatographic and spectroscopic methods. *Anal Lett*, 53 (2020) 984.

9 Arif T, Bhosale JD, Kumar N, Mandal TK, Bendre RS, Lavekar GS & Dabur R, Natural products–antifungal agents derived from plants. *J Asian Nat Prod Res*, 11 (2009) 621.

10 Das BS, Sarangi A, Sahoo A, Jena B, Patnaik G, Rout SS, Sahoo S & Bhattacharya D, Studies on phytoconstituents, antioxidant and antimicrobial activity of *Trachyspermum ammi* seed oil extract with reference to specific foodborne pathogens. *J Essent Oil Bear Plants*, 25 (2022) 1012.

11 Vijayaraghavan K, Nalini SK, Prakash NU & Madhankumar D, One step green synthesis of silver nano/microparticles using extracts of *Trachyspermum ammi* and Papaver somniferum. *Colloids Surf B*, 94 (2012) 114.

12 Bawazeer S, Rauf A, Naz H, Shah SUA, Waggas DS, Ali J, Mabkhot YN, Faryal & Ramadan MF, Synthesis, characterization and bioactivity profiling of gold nanoparticles of *Trachyspermum ammi* crude extract. *J Pure Appl Microbiol*, 15 (2021) 667.

13 Qamar N, John P & Bhatti A, Toxicological and anti-rheumatic potential of *Trachyspermum ammi* derived biogenic selenium nanoparticles in arthritic balb/c mice. *Int J Nanomedicine*, 15 (2020) 3497.

14 Kaur H, Bhatnagar A & Tripathi SK, Size Tunable Green Synthesis of silver nanoparticles using *Trachyspermum ammi* (Ajwain) and their effect on a B Cell Line. *J NanoengNanomanuf,* 3 (2013) 154.

15 Khandelwal R, Arora SK, Phase DM, Pareek A & Kant R, Study of antimicrobial activities of green synthesized silver nanoparticles. *J Indian Chem Soc*, 97 (2020) 455.

16 Perveen K, Husain FM, Qais FA, Khan A, Razak S, Afsar T, Alam P, Almajwal AM & Abulmeaty MM, Microwave-assisted rapid green synthesis of gold nanoparticles using seed extract of *Trachyspermum ammi*: ROS mediated biofilm inhibition and anticancer activity. *Biomolecules*, 11 (2021) 197.

17 Chouhan N, Ameta R & Meena RK, Biogenic silver nanoparticles from *Trachyspermum ammi* (Ajwain) seeds extract for catalytic reduction of p-nitrophenol to p-aminophenol in excess of NaBH4. *J Mol Liq*, 230 (2017) 74.

18 Masum MMI, Siddiqa MM, Ali KA, Zhang Y, Abdallah Y, Ibrahim E, Qiu W, Yan C & Li B, Biogenic synthesis of silver nanoparticles using Phyllanthusemblica fruit extract and its inhibitory action against the pathogen Acidovoraxoryzae strain RS-2 of rice bacterial brown stripe. *Front Microbiol*, 10 (2019) 820.

19 Sarkar S & Kotteeswaran V, Green synthesis of silver nanoparticles from aqueous leaf extract of Pomegranate (Punica granatum) and their anticancer activity on human cervical cancer cells. *Adv Nat Sci Nanosci Nanotechnol*, 9 (2018) 025014.

20 Ghagane SC, Puranik SI, Kumbar VM, Nerli RB, Jalalpure SS, Hiremath MB, Neelagund S & Aladakatti R, In vitro antioxidant and anticancer activity of Leea indica leaf extracts on human prostate cancer cell lines. *Integr Med Res*, 6 (2017) 79.

21 Qais FA, Shafiq A, Khan HM, Husain FM, Khan RA, Alenazi B, Alsalme A & Ahmad I, Antibacterial effect of silver nanoparticles synthesized using *Murraya koenigii* (L.) against multidrug-resistant pathogens. *Bioinorg Chem Appl*, 2019 (2019) 4649506.

22 Rautela A & Rani J, Green synthesis of silver nanoparticles from Tectona grandis seeds extract: characterization and mechanism of antimicrobial action on different microorganisms. *J Anal Sci Technol*, 10 (2019) 1.

23 Bhanumathi R, Vimala K, Shanthi K, Thangaraj R & Kannan S, Bioformulation of silver nanoparticles as berberine carrier cum anticancer agent against breast cancer. *New J Chem*, 41 (2017) 14466.

24 Jain J, Arora S, Rajwade JM, Omray P, Khandelwal S & Paknikar KM, Silver nanoparticles in therapeutics: development of an antimicrobial gel formulation for topical use. *Mol Pharm*, 6 (2009) 1388.

25 Abdellatif AA & Tawfeek HM, Transfersomal nanoparticles for enhanced transdermal delivery of clindamycin. *AAPS Pharm Sci Tech*, 17 (2016) 1067.

26 Mashwani ZU, Khan T, Khan MA & Nadhman A, Synthesis in plants and plant extracts of silver nanoparticles with potent antimicrobial properties: current status and future prospects. *Appl Microbiol Biotechnol*, 99 (2015) 9923.

27 Bala A & Rani G, A review on phytosynthesis, affecting factors and characterization techniques of silver nanoparticles designed by green approach. *Int Nano Lett,* 10 (2020) 159.

28 Reddy NV, Li H, Hou T, Bethu MS, Ren Z & Zhang Z, Phytosynthesis of silver nanoparticles using Perilla frutescens leaf extract: characterization and evaluation of antibacterial, antioxidant, and anticancer activities. *Int J Nanomedicine,* 16 (2021) 15.

29 Gomathi AC, Rajarathinam SX, Sadiq AM & Rajeshkumar S, Anticancer activity of silver nanoparticles synthesized using aqueous fruit shell extract of Tamarindus indica on MCF-7 human breast cancer cell line. *J Drug DelivSciTechnol*, 55 (2020) 101376.

30 He Y, Wei F, Ma Z, Zhang H, Yang Q, Yao B, Huang Z, Li J, Zeng C & Zhang Q, Green synthesis of silver nanoparticles using seed extract of Alpinia katsumadai, and their antioxidant, cytotoxicity, and antibacterial activities. *RSC Adv*, 7 (2017) 39842.

31 Mourdikoudis S, Pallares RM & Thanh NT, Characterization techniques for nanoparticles: comparison and complementarity upon studying nanoparticle properties. *Nanoscale*, 10 (2018) 12871.

32 Filippov SK, Khusnutdinov R, Murmiliuk A, Inam W, Zakharova LY, Zhang H & Khutoryanskiy VV, Dynamic light scattering and transmission electron microscopy in drug delivery: A roadmap for correct characterization of nanoparticles and interpretation of results. *Mater Horiz*, 10 (2023) 5354.

33 Khorrami S, Zarrabi A, Khaleghi M, Danaei M & Mozafari MR. Selective cytotoxicity of green synthesized silver nanoparticles against the MCF-7 tumor cell line and their enhanced antioxidant and antimicrobial properties. *Int J Nanomedicine*, 13 (2018) 8013.

34 Javed B, Ikram M, Farooq F, Sultana T, Mashwani ZUR & Raja NI, Biogenesis of silver nanoparticles to treat cancer, diabetes, and microbial infections: A mechanistic overview. *Appl Microbiol Biotechnol*, 105 (2021) 2261.

35 Salari S, Bahabadi SE, Samzadeh-Kermani A & Yosefzaei F, In-vitro evaluation of antioxidant and antibacterial potential of greensynthesized silver nanoparticles using *Prosopis farcta* fruit extract. *Iran J Pharm Res,* 18 (2019) 430.

36. Inbathamizh L, Ponnu TM & Mary EJ, In vitro evaluation of antioxidant and anticancer potential of Morinda pubescens synthesized silver nanoparticles. *J Pharm Res*, 6 (2013) 32.

37 Moodley JS, Krishna SBN, Pillay K, Sershen & Govender P, Green synthesis of silver nanoparticles from Moringa oleifera leaf extracts and its antimicrobial potential. *Adv Nat Sci Nanosci Nanotechnol*, 9 (2018) 015011.

38 Choi JS, Lee JW, Shin UC, Lee MW, Kim DJ & Kim SW, Inhibitory activity of silver nanoparticles synthesized using lycopersiconesculentum against biofilm formation in candida species. *Nanomaterials*, 9 (2019) 1512.

39 Khatoon N, Mishra A, Alam H, Manzoor N & Sardar M, Biosynthesis, characterization, and antifungal activity of the silver nanoparticles against pathogenic *Candida* species. *Bio Nano Sci*, 5 (2015) 65.

40 Durán N, Durán M, De Jesus MB, Seabra AB, Fávaro WJ & Nakazato G, Silver nanoparticles: A new view on mechanistic aspects on antimicrobial activity. *Nanomed Nanotechnol Biol Med*, 12 (2016) 789.

41 Mansoor S, Zahoor I, Baba TR, Padder SA, Bhat ZA, Koul AM & Jiang L, Fabrication of silver nanoparticles against fungal pathogens. *Front nanotechnol*, 3 (2021) 679358.

42 Vazquez-Muñoz R, Meza-Villezcas A, Fournier PGJ, Soria-Castro E, Juarez-Moreno K, Gallego-Hernández AL, Bogdanchikova N, Vazquez-Duhalt R & Huerta-Saquero A, Enhancement of antibiotics antimicrobial activity due to the silver nanoparticles impact on the cell membrane. *PLoS One*, 14 (2019) e0224904.

43 Das P, Dutta T, Manna S, Loganathan S & Basak P, Facile green synthesis of non-genotoxic, non-hemolytic organometallic silver nanoparticles using extract of crushed, wasted, and spent Humuluslupulus (hops): Characterization, anti-bacterial, and anti-cancer studies. *Environ Res*, 204 (2022) 111962.

44 Varaprasad K, Mohan YM, Ravindra S, Reddy NN, Vimala K, Monika K, Sreedhar B & Raju KM, Hydrogel–silver nanoparticle composites: a new generation of antimicrobials. *J Appl Polym Sci*, 115 (2010) 1199.